Bull. Mater. Sci., Vol. 38, No. 7, December 2015, pp. 1705–1709. © Indian Academy of Sciences.

Understanding the impact of graphene sheet tailoring on the conductance of GNRFETs

DEVENDRA UPADHYAY and SUDHANSHU CHOUDHARY*
School of VLSI and Embedded System Design, National Institute of Technology, Kurukshetra 136119, India

MS received 1 May 2015; accepted 13 July 2015

Abstract. **The effect of tailoring the graphene sheets used as channel in a graphene nanoribbon field effect transistor (GNRFET) was investigated. The study was performed using self-consistent solution of Poisson's and Schrodinger's equation in combination with non-equilibrium Green's function (NEGF) formalism. Graphene sheet channel was tailored into different shapes and found that with the introduction of edge roughness along the border of GNR sheet the bandgap of GNRFET channel increases. Tailoring the channel decreases mobility and transmission probability to a great extent and thus the performance of *I–V* characteristics of GNRFET degrades.**

Keywords. **Graphene; nanoribbon; FET; non-equilibrium Green's function.**

1. Introduction

With the progress in nanotechnology research, it is possible to think about silicon transistors in the sub-100 nm regime. However, increased short channel effect, severe process parameter variations and increasing leakage current remain a challenge for the device and circuit designers. In an attempt to counter these problems associated with the scaling of silicon transistors, researchers are looking for alternate materials for post-Si nanoelectronics era. Of the different materials explored so far graphene seems to be most promising candidate due to its extraordinary properties.[1,2]

Graphene is a two-dimensional (2D) sheet of carbon (C) atoms bound together in a honeycomb-like structure in which each carbon is sp^2-hybridized and connected with three adjacent C-atoms.[3] Electrons in graphene behave as massless fermions and travel through the lattice with long mean free paths and possess very high mobility of 27,000 $cm^2\ v^{-1}\ s^{-1}$.[4] However, the main issue with this technology is that graphene has zero bandgap. This makes it less desirable for transistor applications. Lately, researchers found that bandgap can be introduced by laterally confining the graphene sheet into narrow strips of small widths called graphene nanoribbons (GNRs).[5] Previously reported theoretical works show energy gap of GNR is inversely proportional to their width and due to their reduced dimensions edge states play an important role defining non-null energy gap for all ribbon widths.[6] Graphene transistor can be created by connecting the GNR channel to metal contacts which forms Schottky barrier transistor or by doping the drain and source extension to have MOSFET-like operation.[7]

In the previous studies, it has been reported that nanodevices (in the sub-10 nm range) like GNR field transistor (GNRFET) and carbon nanotube FET (CNTFET) do not saturate.[8,9] It also becomes difficult to turn OFF graphene FETs because of zero bandgap of the GNR sheet channel. It has also been reported previously that defects can affect the band gap in GNR sheet.[10] Therefore, it is of interest to explore the effect of tailored GNR sheets in the GNRFET channel. The objective of the investigation remains in finding a way to saturate and turn off the transistor.

One of the most prevalent ways of analysing the performance of any transistor is through the various currents observed with different parameters and conditions. In particular, if I_{DS}, V_{DS} and V_{GS} are the drain-to-source current, drain-to-source voltage and gate-to-source voltage, respectively, and V_{DD} is the power supply, transfer characteristics plot of I_{DS} *vs.* V_{GS} helps us in determining off current I_{off} with $I_{off} = I_{DS}$ for $V_{DS} = V_{DD}$ and $V_{GS} = 0$ V. On the other hand output characteristics plot of I_{DS} *vs.* V_{DS} of any device helps to determine on current I_{on} with $I_{on} = I_{DS}$ for $V_{DS} = V_{DD}$ and $V_{GS} = V_{DD}$. These two currents and their ratios are the most desired parameters to be improved for better transistor operation.

In this paper, GNR MOSFET with different channel widths and channel dimensions (based on N, as shown in figure 1) using NanoTCADViDES software was studied.[11] The behaviour of GNRFET with its channel tailored into different shapes and different widths was investigated. From this study, it was found that edge roughness can greatly affect device electrical performance, as reported in sections ahead.

2. Materials and method

The simulations are based on self-consistent solution of the Poisson and Schrodinger equations in combination with non-equilibrium Green's function (NEGF) formalism.[12,13]

*Author for correspondence (hellosudhanshubit@gmail.com)

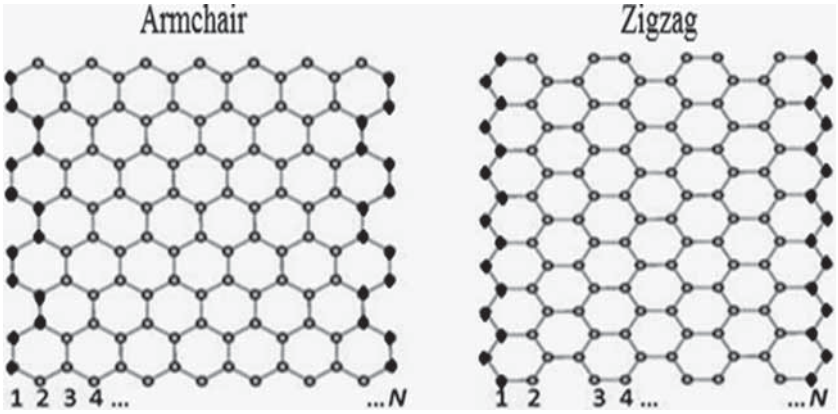

Figure 1. Schematic of types of GNR with dark dots on the vertical edges showing (**a**) armchair and (**b**) zigzag GNR. Along the horizontal axis N is the number of dimer lines along the width for AGNR and number of zigzag chains along the width for ZGNR. AGNR was used throughout the text so N denotes the number of dimer lines.

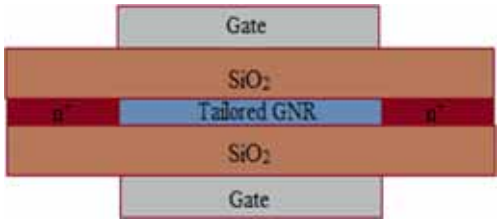

Figure 2. Device structure of MOSFET with doped source and drain extensions. The SiO_2 gate insulator is 1.5 nm thick with a relative dielectric constant $\kappa = 3.9$. Tailored GNR channel of different widths and shapes as shown in figure 3 are used.

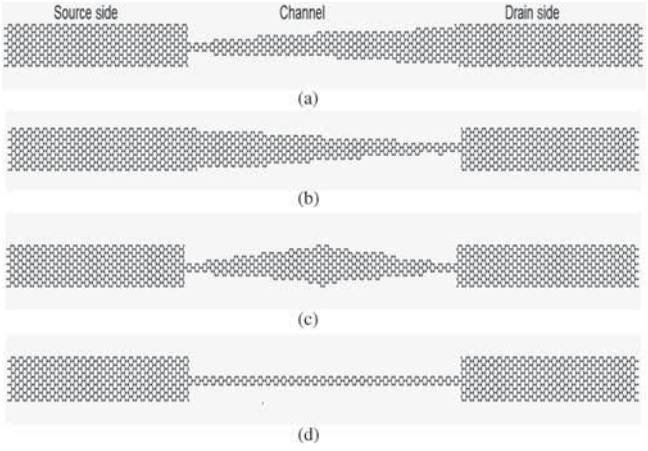

Figure 3. Tailored channel in different shapes: (**a**) channel tailored from source side, (**b**) channel tailored from drain side, (**c**) channel tailored from both sides and (**d**) channel tailored into H shape.

NanoTCADViDES software[11] was used to compute transport in GNRFETs. The electron and hole concentrations are computed by solving the Schrodinger equation with open boundary conditions, by means of the NEGF formalism. A tight-binding Hamiltonian with an atomistic (p_z orbitals)

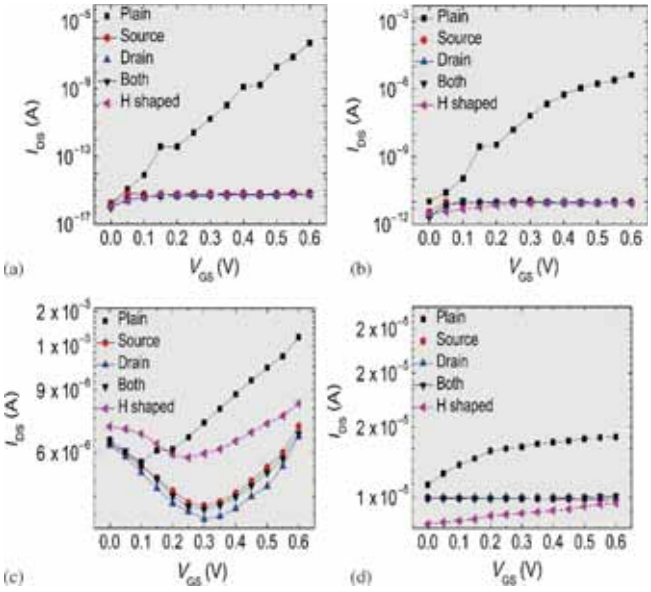

Figure 4. Transfer characteristics of GNRFET with channel tailored into different shapes (as shown in figure 3) is compared with plain GNR sheet with N as 10, 12, 14 and 26, in (**a**), (**b**), (**c**) and (**d**) of this figure. For all simulations V_{DS} is 0.2 V.

basis has been used with real space approach. Green's function can be expressed as[13]

$$G(E) = \left[EI - H - \sum\nolimits_{S} - \sum\nolimits_{D}\right]^{-1},$$

where E is the energy, I the identity matrix, H the Hamiltonian of the GNR, and $\sum_S$ and $\sum_D$ the self-energies of the source and drain, respectively. As can be seen, transport is assumed to be completely ballistic. The GNRs considered are all of armchair type. A point charge approximation is assumed, where all the free charge around each carbon atom is spread with a uniform concentration in the elementary cell including the atom.

Assuming that the chemical potentials of the reservoirs are aligned at the equilibrium with the Fermi level of the GNR,

and given that there are no fully confined states, the electron concentration is given as[13]

$$n(\vec{r}) = 2\int_{E_t}^{+\infty} \mathrm{d}E[||\psi_S(E,\vec{r})|^2 f(E-E_{F_S}) + |\psi_D(E,\vec{r})|^2 f(E-E_{F_D})],$$

while the hole concentration is[13]

$$p(\vec{r}) = 2\int_{-\infty}^{E_T} \mathrm{d}E\{||\psi_S(E,\vec{r})|^2 [1-f(E-E_{F_S})] + |\psi_D(E,\vec{r})|^2 [1-f(E-E_{F_D})]\},$$

where $\vec{r}$ is the coordinate of the carbon site, f the Fermi–Dirac occupation factor, and $|\psi_S|^2$ ($|\psi_D|^2$) the probability that states injected by the source (drain) reach the carbon site ($\vec{r}$), and E_{F_S} (E_{F_D}) is the Fermi level of the source (drain).

The current has been computed as[14]

$$I = \frac{2q}{h}\int_{-\infty}^{+\infty} \mathrm{d}E\, T(E)[f(E-E_{F_S}) - f(E-E_{F_D})],$$

where q is the electron charge, h Planck's constant, and $T(E)$ is the transmission coefficient where Tr is the trace operator[13]

$$T(E) = -\mathrm{Tr}\left[\left(\sum\nolimits_S - \sum\nolimits_S^{\dagger}\right) G \left(\sum\nolimits_D - \sum\nolimits_D^{\dagger}\right) G^{\dagger}\right].$$

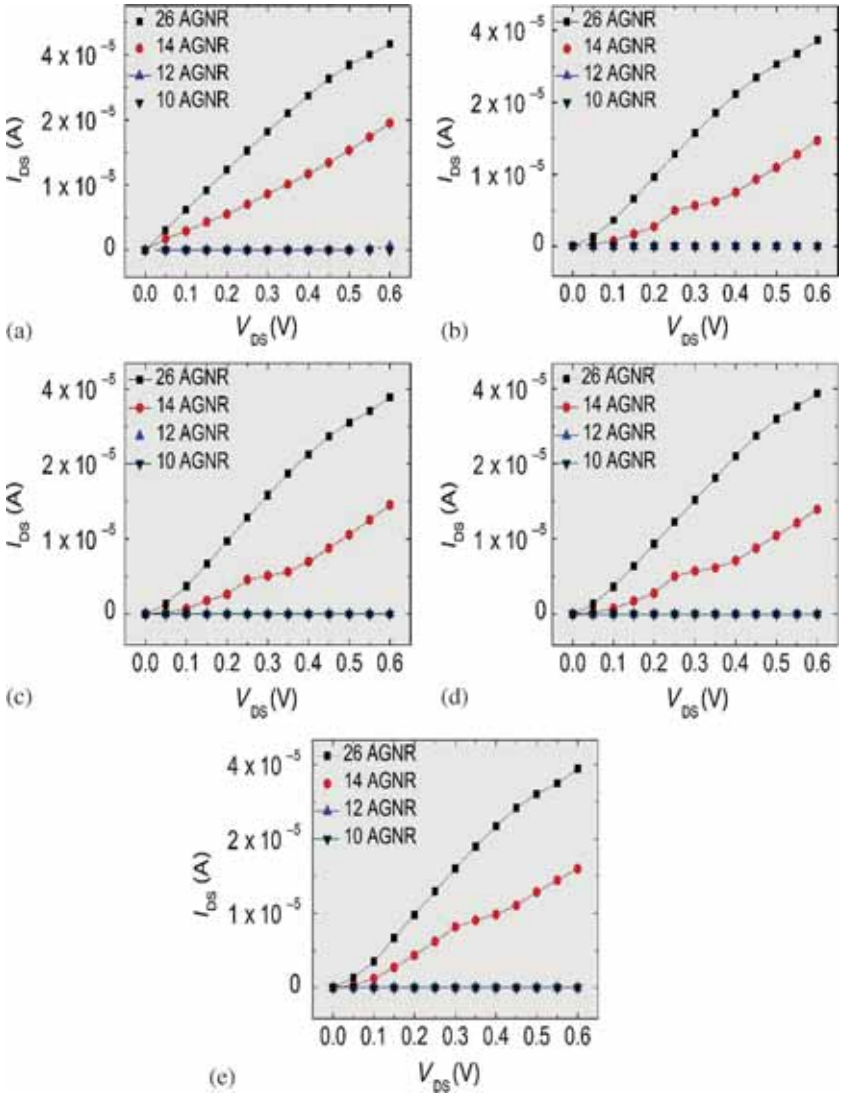

Figure 5. Output characteristics of GNR channel with (**a**) untailored or plain sheet, (**b**) tailored from source side, (**c**) tailored from drain side, (**d**) tailored from both sides and (**e**) tailored into H shape, for different GNR widths with $N = 26$, 14, 12 and 10. For all simulations V_{GS} is 0.2 V.

2.1 *Simulation set-up for studying the effect of tailoring the graphene sheet channel*

Double gated geometry is used for the device as shown in figure 2. The gate oxide ($\kappa = 3.9$) is SiO_2 that has a thickness of 1.5 nm, the lateral spacing S is equal to 1 nm. Source and drain are doped extension of the GNR's channel with a molar fraction equal to 5×10^{-3}. Doping is carried out uniformly. The channel is 15 nm while source and drain extensions are 10 nm long in all the simulations. Ballistic transport is assumed. The power supply voltage V_{DD} is 0.2 V, room temperature T is 300 K. Edge bond relaxation is treated according to *ab initio* calculation, and a tight-binding parameter of $t_0 = 2.7$ eV is used.

The simulations are carried out for GNRFET with channel tailored into different shapes. The channel is tailored from source side, drain side, both side, and H shaped as shown in (a–d) of figure 3. Each of the tailored configurations of channel is tried with different widths of armchair GNR (AGNR) as shown in figure 1a with N as 10, 12, 14 and 26.

3. Results and discussion

In today's scenario, GNRs with varying widths can be manufactured either by patterning epitaxially grown graphene or by cutting mechanically exfoliated graphene. However as graphene is cut into GNRs of different widths through lateral confinement it is realized that it shows an oscillating behaviour in terms of bandgap as width is changed.[15] The bandgap of GNR increases as its width decreases. This property was also observed through the results of the simulations on AGNR of various widths. Furthermore, this GNR was tailored into various shapes and thus introduced edge roughness along the edges. It was observed that minimal edge disorder can induce the conduction energy gap in the otherwise metallic GNRs. The formation of the conduction gap has been related to the edge disorder-induced Anderson-type localization which leads to formation of surface-like states, strongly enhanced density of states at the edges, and blocking of conductive paths through the ribbons.[16] The Anderson localization leads to degradation of mobility in tailored GNR.[7] Because of the decrease in mobility the transistor shows very low OFF current in case of 10 AGNR and 12 AGNR (see figure 4a and b) whereas for 14 AGNR and 26 AGNR transistor remains ON at even $V_{GS} = 0$ V (see figure 4c and d). Transfer characteristics in figure 4 and output characteristics in figure 5 for AGNR of different widths shows that tailoring degrades the transistor performance because edge roughness provides gap states induced in the bandgap region, which further increases the leakage current at the OFF state in a transistor.

Bandgaps in AGNRs have been categorized into three main categories as $N = 3z + 1$, $3z + 2$, $3z$ (where N is number of dimer lines and z is a positive integer) and through local density approximation (LDA) calculation energy gap hierarchy is $E_G^{3z+1} > E_G^{3z} > E_G^{3z+2} (\neq 0)$.[17] In the simulations of GNR with different widths of $N = 12$ ($3z$), 10 ($3z+1$), 14, and 26 ($3z+2$), the same hierarchy was observed in energy gap, as shown in figure 6. The transmission coefficient of plain sheet shows that energy gap of 14 AGNR and 26 AGNR is close to zero. In total 10 AGNR has maximum energy gap while 12 AGNR has a bandgap in between (14, 26) AGNR and 10 AGNR. Therefore, due to less energy gap, 26 AGNR and 14 AGNR show desirable output characteristics while 12 AGNR and 10 AGNR result in low currents due to high energy gap which further results in nearly zero current for all tailored channel shapes (see figure 5). With tailoring of channel, it can be observed that bandgap has increased and transmission probability of electron from source to drain has also decreased (see figure 6). This also explains the reason behind low OFF current for 10

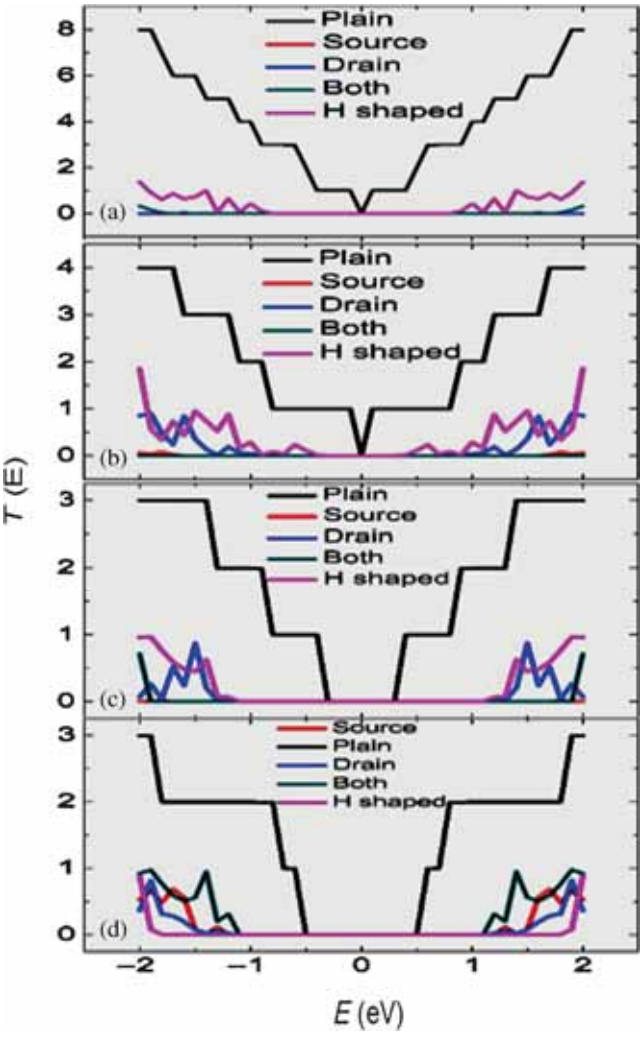

Figure 6. Energy [E] *vs.* transmission coefficient [$T(E)$] plot for different widths of AGNR having channel tailored into different shapes as shown in figure 2, and is compared with plain GNR sheet having different widths with N as 26, 14, 12 and 10 in (**a**), (**b**), (**c**) and (**d**) of this figure.

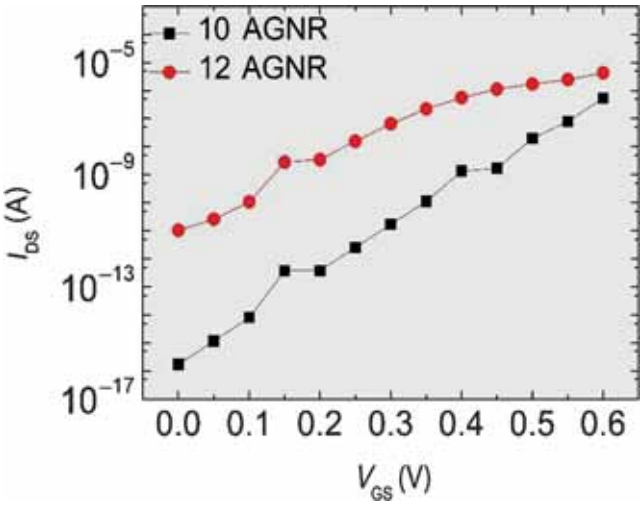

Figure 7. Transfer characteristics of 10 AGNR and 12 AGNR for untailored channel with low desirable off currents.

Table 1. Bandgap variation with AGNR shape and size.

	Bandgap (E_g) (eV)				
GNR type	Plain	Source_side	Drain_side	Both_side	H shape
10 AGNR	0.65	1.510	1.511	1.512	1.49
12 AGNR	0.58	1.2	1.23	1.22	1.21
14 AGNR	0.15	0.16	0.162	0.162	0.166
26 AGNR	0.05	0.055	0.06	0.06	0.07

AGNR and 12 AGNR shown in figures 5 and 7. Furthermore, bandgap variations with AGNR shape are given in table 1.

4. Conclusion

In summary, GNRFET with various GNR sheet channel shapes was investigated and found that with the introduction of edge roughness along the border of GNR sheet the bandgap of GNRFET channel increases. Tailoring the channel decreases mobility and transmission probability to a great extent and thus the performance of I–V characteristics of GNRFET degrades. Thus, with the introduction of tailoring in channel it was observed that overall conductance of GNRFET decreases.

References

1. Geim A K and MacDonald A H 2007 *Phys. Today* **60** 35
2. Novoselov K S, Geim A K, Morozov S V, Jiang D, Zhang Y, Dubonos S V, Grigorieva I V and Firsov A A 2004 *Science* **306** 666
3. Wu Y, Farmer D B, Xia F and Avouris P 2013 *Proc. IEEE* **101** 1620
4. Zhang Y B, Tan Y W, Stormer H L and Kim P 2005 *Nature* **438** 201
5. Han M Y, Ozyilmaz B, Zhang Y B and Kim P 2007 *Phys. Rev. Lett.* **98** 206
6. Nakada K, Fujita M, Dresselhaus G and Dresselhaus M S 1996 *Phys. Rev. B* **54** 17954
7. Yoon Y, Fiori G, Hong S, Iannaccone G and Guo J 2008 *IEEE Trans. Electron. Dev.* **55** 2314
8. Franklin A D, Luisier M, Han S-J, Tulevski G, Breslin C M, Gignac L, Lundstrom M S and Haensch W 2012 *Nano Lett.* 758
9. Franklin A D and Chen Z 2010 *Nat. Nanotechnol.* 858
10. Stan M R, Unluer D, Ghosh A and Tseng F 2009 Graphene devices, interconnect and circuits—challenges and opportunities. in: *ISCAS 2009. IEEE International Symposium on Circuits and Systems* May 2009 p 69
11. Fiori G and Iannaccone G 2007 *IEEE Electron. Dev. Lett.* **28** 760
12. Fiori G and Iannaccone G 2013 *Proc. IEEE* **101** 1653
13. Datta S 2005 Quantum transport—atoms to transistors (Cambridge University Press)
14. Choudhary S, Saini G and Qureshi S 2014 *Mod. Phys. Lett. B (World Scientific Publication)* **28** 1
15. Iannaccone G, Fiori G, Macucci M, Michetti P, Cheli M, Betti A and Marconcini P 2009 Perspectives of graphene nanoelectronics: probing technological options with modeling, in: *Proceedings of IEDM 2009. IEEE Conference Proceedings*: December 2009 (Baltimore, MD, USA) p 245
16. Evaldsson M, Zozoulenko I V, Xu H and Heinzel T 2008 *Phys. Rev. B* **78**
17. Son Y-W, Cohen M L and Louie S G 2006 *Phys. Rev. Lett.* **97**